Click to view poster

Diagenetic Controls on Carbonate Reservoir Quality of Jurassic Middle Marrat Formation in Burgan Field, Kuwait*

Bhaskar Chakrabarti[1], Meshal Al-Wadi[1], Hanan Abu Hebiel[1], and Abdul Mohsen Al-Enezi[1]

Search and Discovery Article #20121 (2011)
Posted November 28, 2011

*Adapted from extended abstract prepared in conjunction with poster presentation at AAPG International Conference and Exhibition, Milan, Italy, October 23-26, 2011

[1]Kuwait Oil Company, Kuwait City, Kuwait (bchakrabarti@kockw.com)

Abstract

Middle Marrat Formation in Kuwait was deposited in an inner ramp setting. It was subsequently modified in near surface and burial diagenetic environments. In the present study an attempt has been made to establish the paragenetic sequence, effect of diagenesis on reservoir quality and delineate reservoir facies.

480 ft of conventional core and 125 thin sections were studied; SEM and XRD analysis were carried out in 10 samples. Subsequently facies and property modeling were carried out to delineate reservoir facies.

Five major facies were identified in Middle Marrat in Burgan: Lime mudstone, wackestone, oncoidal wackestone, dolomitic oncoidal wackestone and packstone. In lime mudstone, wackestone and oncoidal wackestone, bladed, isopachous fibrous high Mg calcite cement formed during shallow marine diagenesis. Subsequent exposure to a meteoric diagenetic environment resulted in leaching of high Mg calcite and aragonite resulting in non-touching moldic pores, aragonite neomorphism and equant calcite cementation. Abundance of kaolinite in XRD analysis could be linked to frequent exposure and induction of meteoric water. Burial diagenesis has resulted in compaction, extensive stylolitization, anhydrite cementation of molds and over dolomitization causing drastic reduction in porosity and very low permeability.

In dolomitic oncoidal wackestones, meteoric diagenesis caused leaching and development of moldic porosity. Matrix replacive euhedral, medium-grained dolomite crystals formed in near surface diagenesis. These dolomites show interconnected intercrystalline matrix porosity (up to15%). In packstone, meteoric diagenesis caused extensive leaching, isopachous cement rims along margins of ooids, and partial equant calcite cementation. Excellent interparticle and moldic porosity (up to 25%) and permeability (100-200 md) developed in this facies.

Paragenetic sequence observed in Middle Marrat is marine bladed, isopachous fibrous high Mg calcite cement, meteoric equant calcite cementation coarsening towards pore center, matrix dolomitization, deep burial baroque dolomite and anhydrite cement. Different facies have reacted differently during diagenesis, which ultimately controls porosity. Porous facies have good permeability, thus making packstone and dolomitic wackestone intervals potential reservoirs. Facies and property maps delineate the area of good reservoir facies. The study helped in Middle Marrat reservoir characterization and delineation.

Introduction

Burgan Field is situated in the southeastern part of Kuwait. It is the largest onshore producing field in Kuwait. Main Burgan structure is a north-south trending dome plunging in four directions and consists of several small culminations. Magwa structure is situated in the north and north-south trending Ahmadi Ridge and Arifjan structure are situated respectively in the east and southeast of Main Burgan structure (Figure 1).The structure is dissected by three sets of faults: north-south, northeast-southwest and east-west. North-south faults are found to be the oldest and the east-west are the youngest. Most of the faults are steeply dipping and mainly cutting across the whole Jurassic section.

Jurassic exploration in the Burgan Field started in 1951 and first oil discovery was made in the early years of the 1980's within Middle Marrat reservoirs. To date a total of six Jurassic wells have penetrated Middle Marrat with significant commercial success. However, all these wells were drilled in the northern and central part of Main Burgan Field (Figure 2), while the southern part of the structure remains unexplored.

Understanding of the Middle Marrat reservoir, prediction of reservoir quality and delineation of reservoir facies in the explored northern part, as well as in the unexplored southern part of the structure, was essential. Detailed study was carried out with cores, e-logs and available data from drilled wells to understand Middle Marrat facies association, depositional environment, key reservoir facies, diagenesis and its effect on reservoir quality. Detailed reservoir descriptions were made and different paragenetic stages were outlined with core thin section studies. Diagenetic episodes responsible for retention, generation and destruction of porosity were identified in different lithofacies. Major porosity types (interparticle, moldic, intercrystalline, intraparticle, etc.) were identified to understand reservoir quality. Based on log character and core facies associations, the Middle Marrat was divided into three broad sequences, the reservoir quality of each sequence was evaluated and reservoir facies correlation was made with the six drilled wells. Subsequently a 3D static model was built to generate facies and porosity maps across the entire Burgan Field.

Middle Marrat Facies Association and Depositional Environment in Burgan Field

Based on detailed core study, five facies associations are interpreted in Middle Marrat. These are Facies Association MMF1, MMF2, MMF3, MMF4 and MMF5. Brief descriptions of each of these units are below.

MMF1: Lime mudstone with peloidal wackestone and packstone interbedded with minor packstone, and minor oolitic grainstone/packstone with interbedded lime mudstone, packstone/wackestone are the major representative facies (Figure 9A and Figure 9B). These facies were deposited in a dominantly shallow inner ramp setting.

MMF2: Slightly dolomitized oncoidal wackestones transitional up into packstones/oolitic packstone (Figure 10A and Figure 10B). Bioturbation is common. Bioturbated oncoidal wackestone facies represent deposition in an inner ramp setting in a probable shallow lagoon. Packstones/oolitic packstone deposited in shifting shoals in a shallow inner ramp setting.

MMF3: Lime mudstone, oncoidal wackestone with rare dolomitization of wackestone (Figure 11A and Figure 11B). Limited biodiversity indicates that the lime mudstones were most likely deposited in a restricted, possibly lagoonal environment. Wackestone facies represent deposition in deeper subtidal lagoonal environments affected by gentle currents that were able to periodically move oncoidal grains.

MMF4: Moderately bioturbated lime mudstones with minor wackestone beds containing pyritized dark grains, and algal laminate are characteristics (Figure 12A and Figure 12B).
The lime mudstones are deposited under quiet low energy conditions in a shallow inner shelf lagoonal environment. Microbial laminate facies were likely deposited at the edges of these shallow lagoons.

MMF5: Bioturbated, locally slightly dolomitic oncoidal wackestones with minor packstones and interbeds of lime mudstone are key features (Figure 13A and Figure 13B). Rooted horizons and exposure surfaces are occasional. The oncoidal wackestone facies were likely deposited in a shallow inner shelf environment. Interbedded lime mudstone facies were deposited under quiet subtidal conditions in inner shelf lagoonal environments. The environment became emergent with development of exposure surfaces, intraclastic horizons, fissures and rootlets.

Middle Marrat Diagenesis

The earliest diagenesis consisting of hardground formation and synsedimentary pyritization occurred within the marine environment. These include precipitation of several types of marine cements (Figure 14A and Figure 14C) (bladed rims, and micrite cement) and the development of multiple hardgrounds. It is believed that below the water-sediment interface, with the possible exception of active shoals, most of the sediments were anoxic. This is reflected by typical redox stains within shallow-water sediments.

The next phase of diagenesis (that may have occurred more than once within the Middle Marrat) is related to subaerial exposure. Exposure is caused by relative uplift, but that may simply involve lowstand sea levels rather than tectonics. Exposure surfaces and near-exposure surfaces were related to meteoric diagenesis including leaching, in filtering of soil clays (Figure 16A) and early rim cement of fine equant calcite. Further, there is evidence for erosion of clasts and soil development (Figure 16A) during exposure. This is typical of early meteoric diagenesis related to exposure.

Matrix dolomitization (Figure 15A, B and C) matrix neomorphism (Figure 17A) and coarse-equant calcite (Figure 14C) may have occurred within the late meteoric zone or they may, in part, represent shallow subsurface diagenesis. Some leaching was fabric selective (creating moldic pores) and some leaching was not fabric selective (Figure 14A). Matrix dolomitization and matrix recrystallization created intercrystalline matrix porosity.

The remaining diagenetic phases most likely occurred within the subsurface diagenetic setting. Medium to coarse equant calcite cement pre-dates baroque dolomite precipitation (Figure 14B and C). Anhydrite is believed to have preceded baroque dolomite and precipitated primarily as a replacement mineral (Figure 16B) within the shallow subsurface. The late stages of diagenesis consist of medium to coarse crystalline, euhedral pyrite and hydrocarbon migration with the development of bitumen cement (Figure 15C). Within the currently available dataset it appears that fractures began to form very early, probably within the marine cements and hardgrounds. Some fractures were inherited within eroded clasts, while other relatively early fractures (Figure 17B and C) were involved in early compaction.

Later-stage compaction crushed moldic ooids, created stylolites, and may have locally generated a small amount of coarse crystalline calcite cement. The stages of paragenetic sequences of Middle Marrat are shown in Figure 3. There are three phases of leaching recognized in the Middle Marrat Formation thin sections. First is related to exposure through “uplift” or sea level fall and establishment of meteoric conditions. The second leaching phase appears to have occurred just before the precipitation of baroque dolomite within the shallow to deep subsurface. Based on the relative timing of phases identified within the Marrat thin sections, the second phase of leaching, probably in concert with matrix dolomitization, was responsible for intercrystalline matrix porosity and small, non-touching moldic porosity. A third phase of very minor leaching was related to the migration of organic acids at the time of hydrocarbon migration.

Diagenesis and Reservoir Quality of Middle Marrat

Facies association MMF5 has minimal reservoir quality except for occasional development of non-touching moldic pores within packstone. Fracture porosity is often observed.

In facies association MMF4 any potential matrix porosity appears to have been virtually destroyed by compaction, over-dolomitization and anhydrite cements (Figure 19D). Reservoir potential is low.

Visual analysis of thin sections of MMF3 does not show a significant improvement in porosity within dolomitic wackestone compared to the tight lime mudstone facies (Figure 19C). Reservoir potential is essentially non-existent for this interval.

In MMF2 intercrystalline matrix porosity (Figure 19B) within oncoid wackestones is in the range of 10-15% and appears to be well connected. Moreover, within packstone early calcite cement propped open the interparticle (Figure 20D) pore system in some areas. Intraparticle porosity is also observed within packstone (Figure 19A). It has good reservoir potential as long as the well-connected interparticle pore system extends laterally.

In MMF1, concurrences of intercrystalline matrix porosity, moldic porosity and interparticle porosity (Figure 20A and B) have been noticed locally. Recrystallization (neomorphism) of the matrix has provided a good intercrystalline pore system (Figure 20C). It is considered to have good potential reservoir quality. Figure 8 summarizes Middle Marrat Facies Association, depositional environment, diagenesis and reservoir potential of Middle Marrat in Burgan Field.

Sequence Stratigraphy, Facies Correlation and Reservoir potential of Middle Marrat in Burgan Field

Middle Marrat in Burgan Field is divided into three sequences based on log character and facies association and each sequence is given a zone name: MM1, MM2 and MM3 from top to bottom (Figure 4). A correlation (Figure 5) is made with drilled wells to understand facies associations and key reservoirs within each zone. It is observed that facies associations MMF1, 2 and 3 are related to zone MM2, and facies association MMF4 and MMF5 are related to zone MM3. Zone MM1 is argillaceous with minor wackestone, packstone intercalation with anhydrite. No core is taken in this zone and thus facies association is mainly derived from cuttings sample information. As discussed in the earlier section, from a reservoir point of view facies associations MMF1 and MMF2 are the best quality, hence zone MM2 has the best reservoir potential. The upper part of MM2 with peloidal packstone and dolomitic oncoidal wackestone has the best reservoir quality with 15% to 20% core porosity. The bottom part of MM2 has no reservoir potential. Zone MM3 has marginal interest from a reservoir point of view. Its facies association MMF4 has poor reservoir quality. The lower part of MM3 has moderate to poor reservoir potential within packstone and wackestone (MMF5). Zone MM1 has negligible interest from a reservoir point of view as observed on e-logs.

3D Static Model and Middle Marrat Reservoir Delineation

A total of five key facies were populated stochastically in the static model using Sequential Indicator Simulation to generate the facies model of the Middle Marrat across the entire Burgan Field. A north-south cross section in Figure 6 shows the facies model of the most important zone MM2 along Burgan Field. Packstone layers are discontinuous, patchy towards the south of the field, while dolomitic wackestone layers are more or less continuous. In the northern part of the field, layers of key reservoir facies (packstone and dolomitic wackestone) are thicker, while towards the south these layers thin.

Facies porosity was populated stochastically using Sequential Gausian Simulation. A north-south cross section in Figure 7 shows the porosity model of the most important zone MM2 across Burgan Field. It is observed that the best porous layers are in the northern part of the field, while in the southern part porosity is moderate to good (Figure 7).

Conclusions

In the present study an attempt has been made to characterize near-surface/vadose, meteoric, marine, shallow and deep burial diagenetic processes which have modified the primary depositional texture of different lithofacies of Middle Marrat Formation in Burgan Field. Fabric selective leaching and matrix dolomitization are major diagenetic processes that have resulted in well-connected interparticle porosity, moldic, intraparticle porosity and intercrystalline matrix porosity. Over dolomitization, medium to coarse equant calcite cementation,

baroque dolomite precipitation, anhydrite replacement, bitumen cementation subsequent to hydrocarbon migration and compaction have resulted in partial to complete destruction of primary porosity. Different lithofacies of Middle Marrat were subjected to more than one type of diagenetic environment/processes and imprints of these episodes were interpreted and different paragenetic episodes were established.

Whole core study enabled interpretation of five major facies associations within Middle Marrat Formation in Burgan Field. Facies associations MMF1 and MMF2 have undergone positive effects of diagenesis and the best porous layers were interpreted within peloidal packstone in MMF1 and dolomitic wackestone in MMF2. Well-connected intraparticle porosity in packstone and intercrystalline matrix porosity between dolomite crystals in dolomitic wackestone have resulted in the best reservoir potential within these two facies. Out of three interpreted sequences within Middle Marrat, Sequence 2 (Zone MM2) has the best reservoir potential in its upper part, developed in packstone and dolomitic wackestone. The lower part of MM2 has no reservoir potential developed within MMF3 facies association. Diagenetic processes such as over dolomitized matrix, anhydrite replacement, coarse dolomite cement and compaction has resulted in complete destruction of porosity. Sequence 3 (Zone MM3) has two facies associations MMF4 in the upper part and MMF5 in the lower part. MMF4 has poor reservoir potential. MMF5 has moderate reservoir potential within packstone. Moldic and intraparticle pores are major pore types within packstone. No cores are available for Sequence 1 (Zone MM1) and hence its reservoir potential is interpreted from e-log interpretation. This zone has marginal reservoir potential.

In an attempt to understand facies variation and predict reservoir quality of Middle Marrat in the unexplored southern part of Main Burgan Field, stochastic facies and porosity models were built. Generated facies and porosity models of Zone MM2 has been discussed in this paper. Continuity of key reservoir facies packstone and dolomitic wackestone layers are predicted towards the southern part of Burgan Field. The porosity model predicts good porosity development within packstone and dolomitic wackestone. This study has played a major role towards Middle Marrat exploration in the southern part of Main Burgan Field.

Acknowledgements

The authors would like to thank Manager of Exploration, KOC, Mr. Ahmed Al-Eidan and Team Leader Prospect Evaluation, KOC, Mr. Mohammed Dawwas Al-Ajmi for their critical review of the study and continuous encouragement. The authors would like thank Ministry of Oil (MOO), Kuwait for giving permission to submit this paper to AAPG. The authors would like to extend their gratitude to Exploration Studies Team, KOC for whole core and thin section analyses and photographs. The authors would also like to thank all reviewers of this paper and to all those who directly or indirectly helped us in completion of the study.

References

Al-Husseini, M.I., 1997, Jurassic sequence stratigraphy of the Western and Southern Arabian Gulf: GeoArabia, v. 2, p. 361-382.

Choquette, P.W., and L.C. Pray, 1970, Geologic nomenclature and classification of porosity in sedimentary carbonates: AAPG Bulletin, v. 54, p. 207-250.

Dunham, R.J., 1962, Classification of carbonate rocks according to depositional texture, *in* Ham (Ed), Classification of Carbonate Rocks, AAPG Memoir 1, p. 108-121.

Yousif, S., and G. Nouman, 1997, Jurassic geology of Kuwait: GeoArabia, v. 2, p. 91-110.

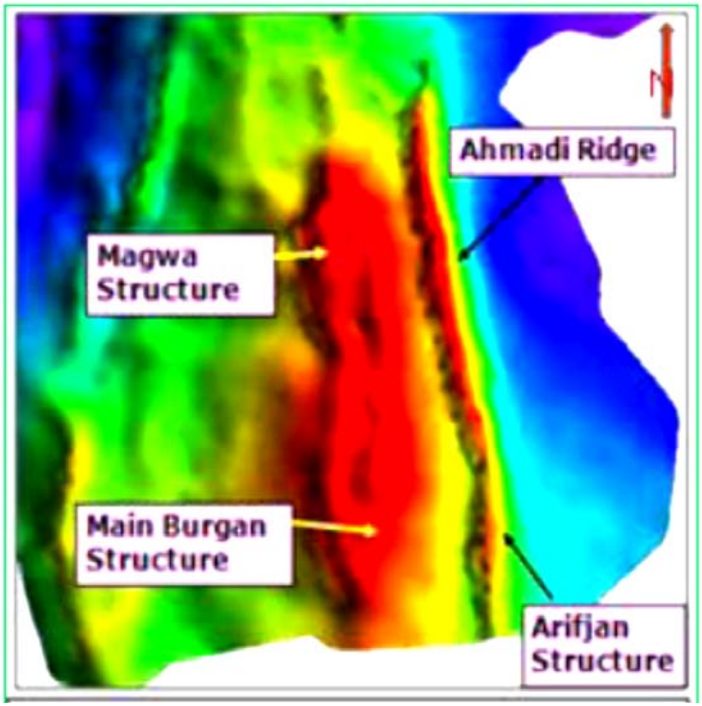

Figure 1. Structural elements adjacent to Main Burgan Field.

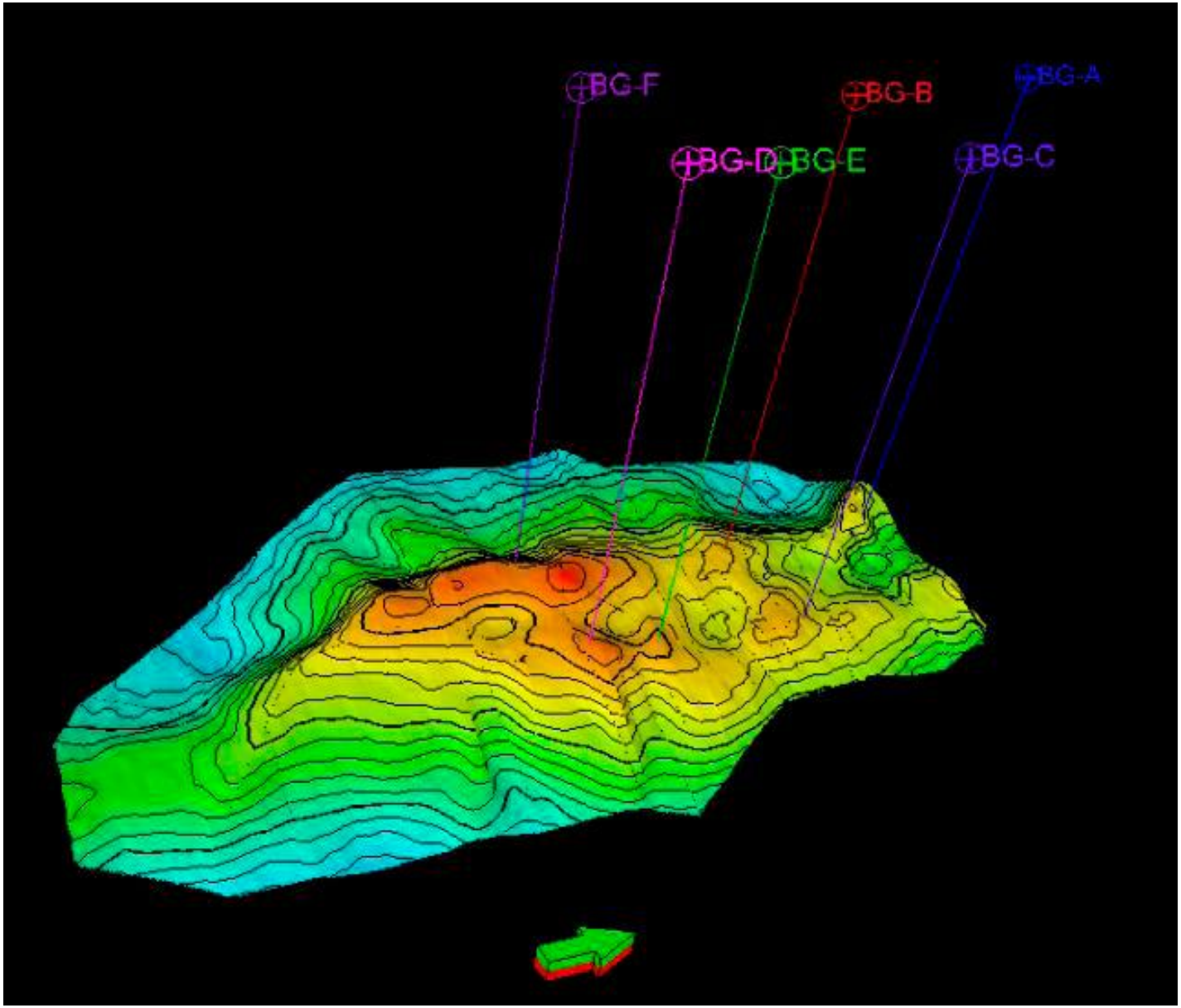

Figure 2. 3D view of Middle Marrat depth horizon along with drilled wells BG-A, B, C, D, E and F in Main Burgan Field.

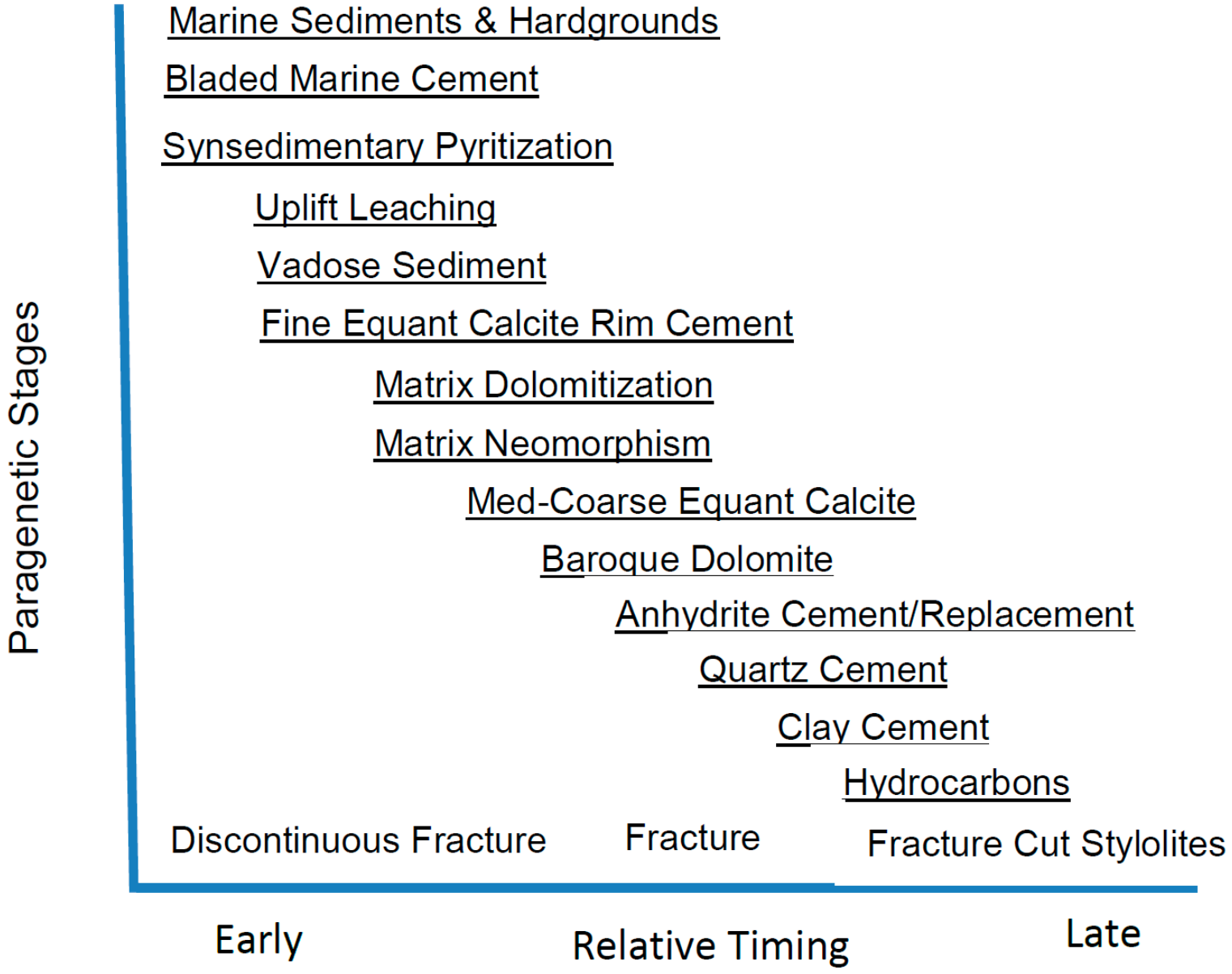

Figure 3. Interpreted paragenetic stages of Middle Marrat.

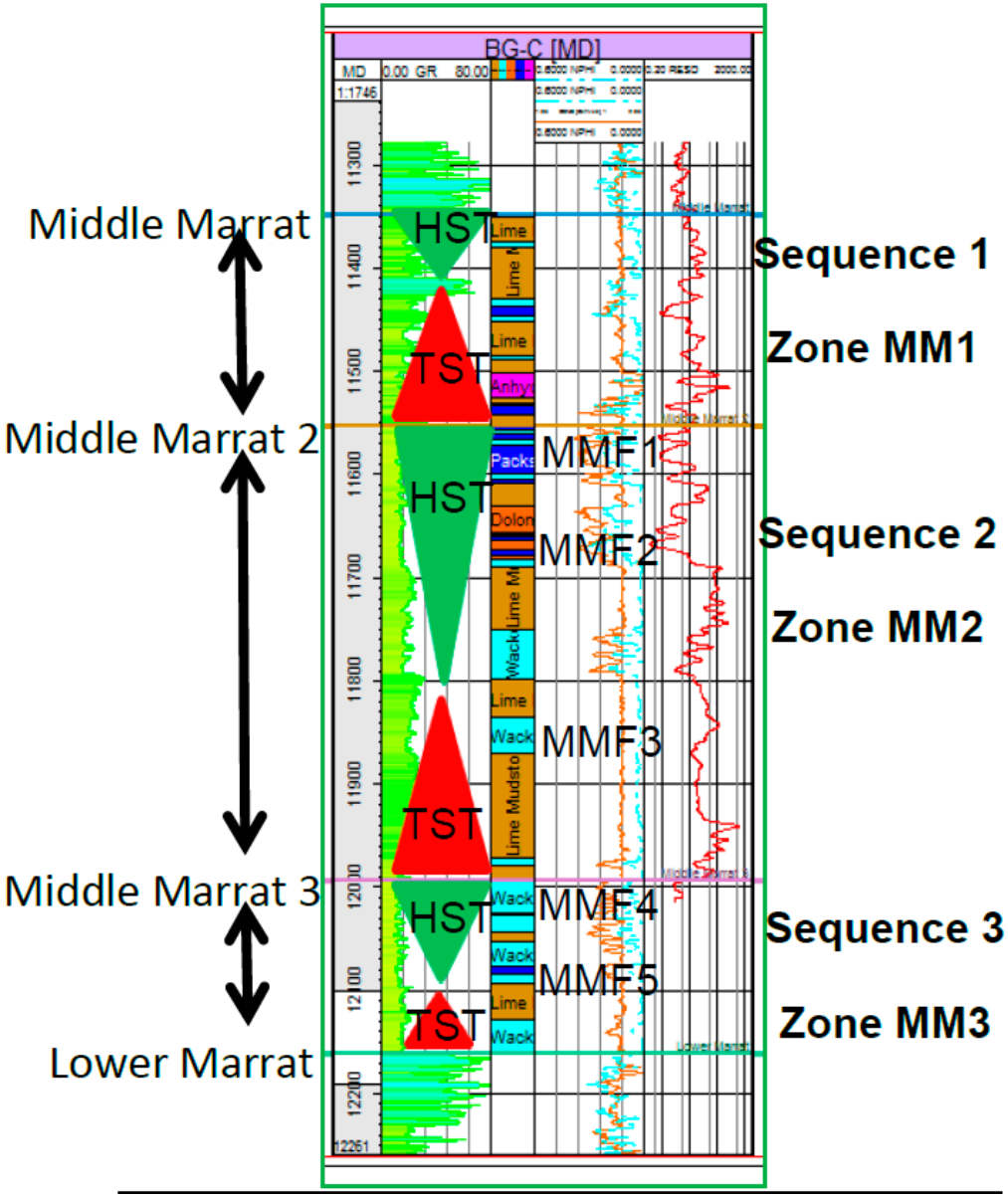

Figure 4. Sequence stratigraphic framework and facies association.

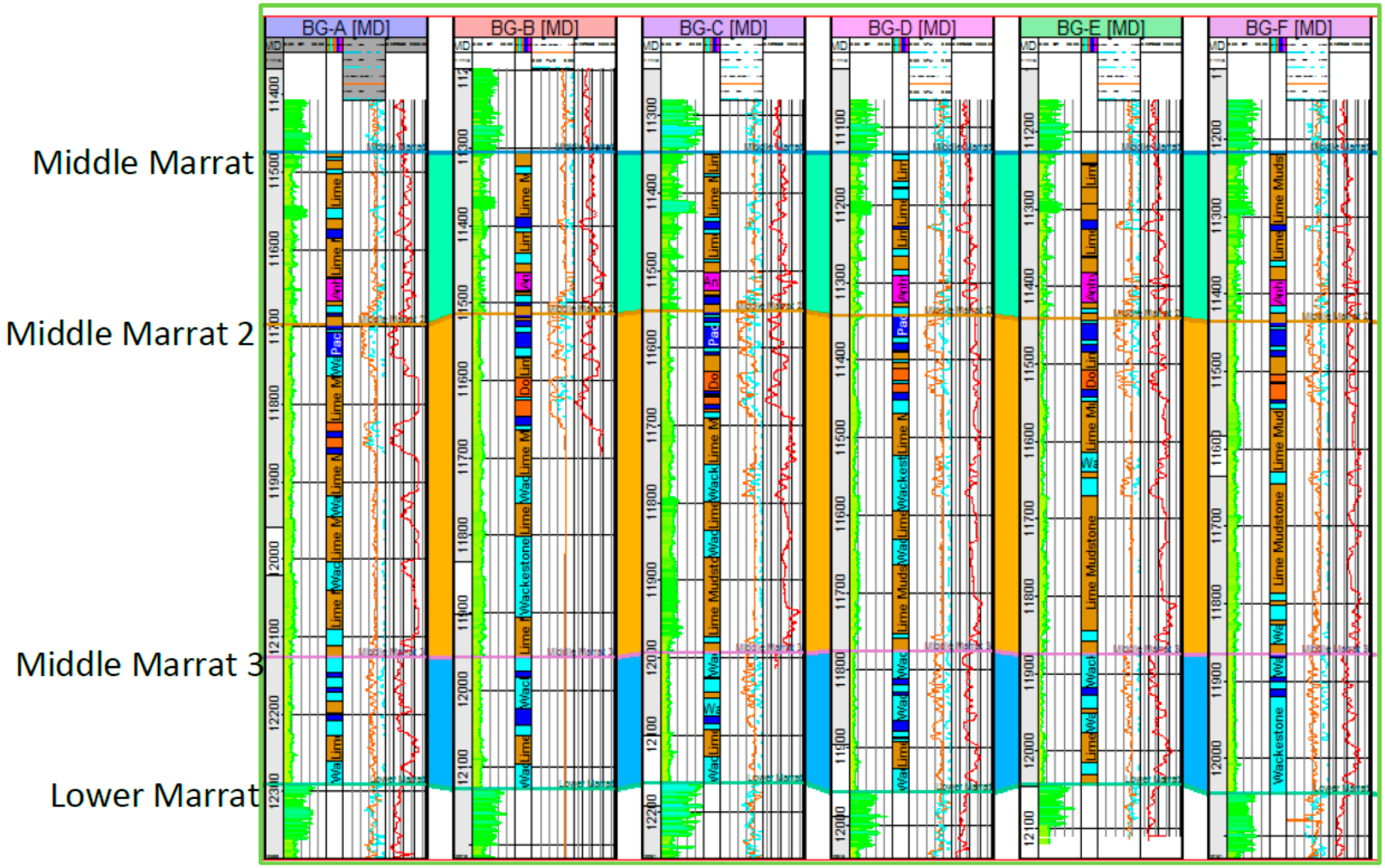

Figure 5. Correlation of Middle Marrat in Burgan Field, continuity of reservoir facies is observed. Note: Section is flattened at Middle Top.

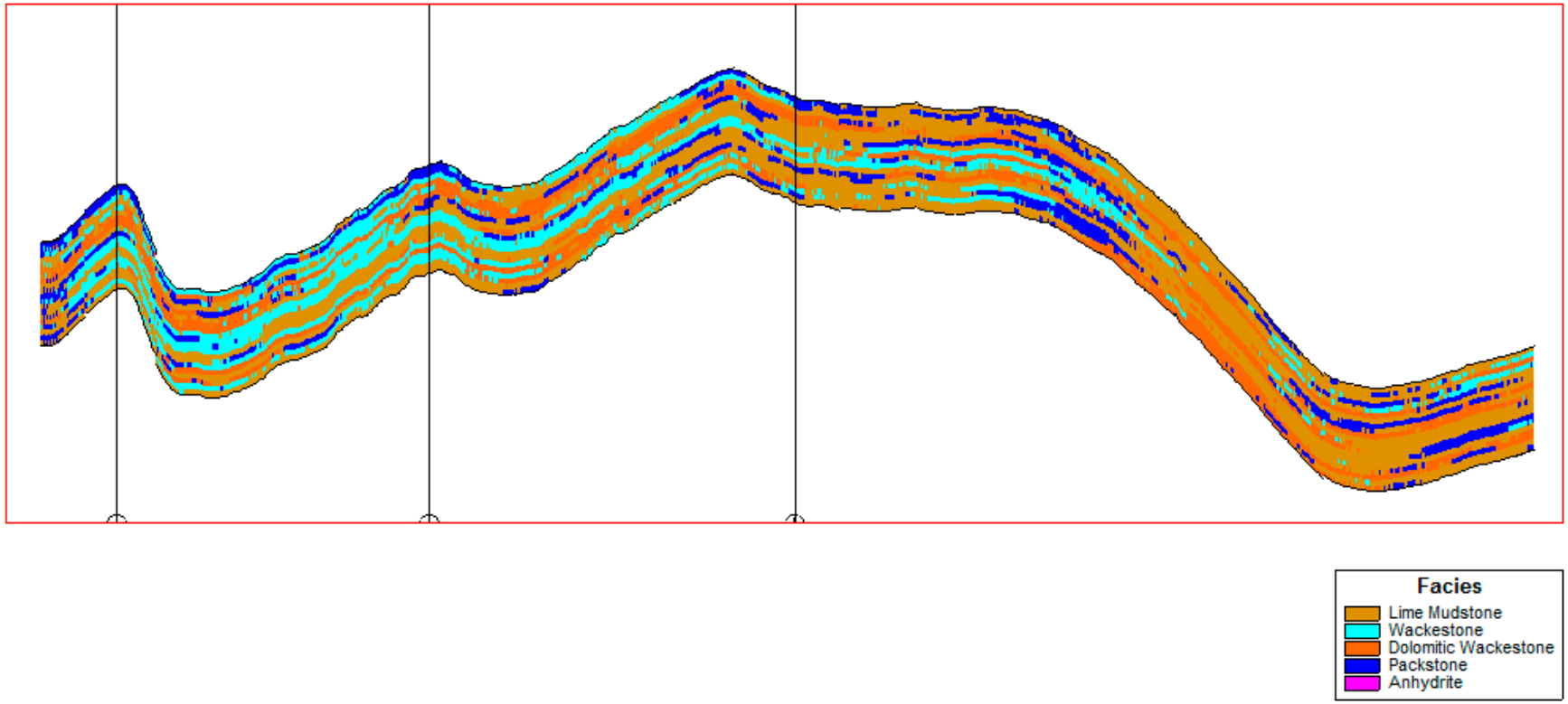

Figure 6. N-S cross section showing facies model of zone MM2 across Burgan Field.

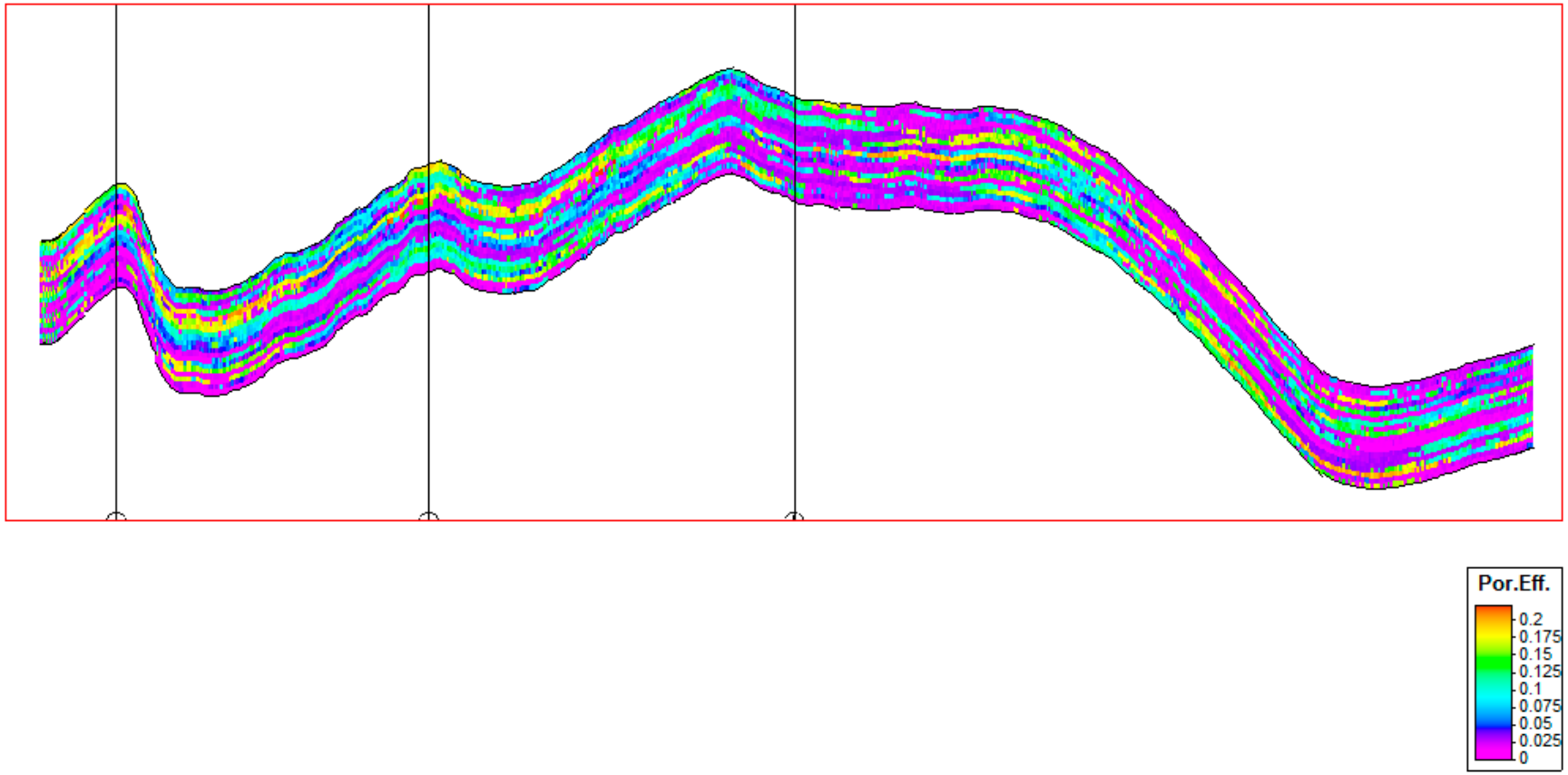

Figure 7. N-S cross section showing porosity model of zone MM2 across Burgan Field.

Formation	Facies Association	Depositional Environment	Diagenetic Control on Reservoir	Pore Types	Reservoir Quality	Visual Porosity
Middle Marrat	MMF1	Inner to mid ramp, occasionally low energy shoal flank	Leaching of grains and matrix neomorphism	Interparticle, moldic, intercrystalline	Excellent to good	Average 20%, Locally 30%
			Hard ground, marine cementation, cementation of all porosities	Fracture, moldic, rarely interparticle	Poor	Average < 1%
	MMF2	Inner ramp	Fabric selective leaching, marine cementation, sub equant sparry calcite cementation	Interparticle, moldic, intraparticle	Good to excellent	Average 10-15%, Locally 20%
			Matrix Dolomitization, Over Dolomitization, compaction	Intercrystalline matrix porosity, moldic	Moderate to good	Average 6-8%, Locally 15%
	MMF3	Inner ramp / Lagoon	Over dolomitized matrix, Anhydrite replacement, coarse dolomite cement, compaction, fracture, matrix dolomitization	Fracture, moldic, intraparticle, occasionally intercrystalline	Very poor	<1%
	MMF4	Mid ramp, Shallow restricted lagoon	Matrix recrystallization, Micro stylolite, Algal laminate, Anhydrite nodules	Fracture, moldic, intercrystalline matrix, intraparticle	Poor	Average 1-2%
	MMF5	Inner ramp	Compaction, Over dolomitization, Anhydrite replacement, multiple stages of fracture filling	Fracture, intraparticle, moldic, intercrystalline within dolomite	Moderate to Poor	Average 2-3%, locally up to 5%

Figure 8. Summary of Middle Marrat facies associations, depositional environments, diagenesis, and reservoir quality.

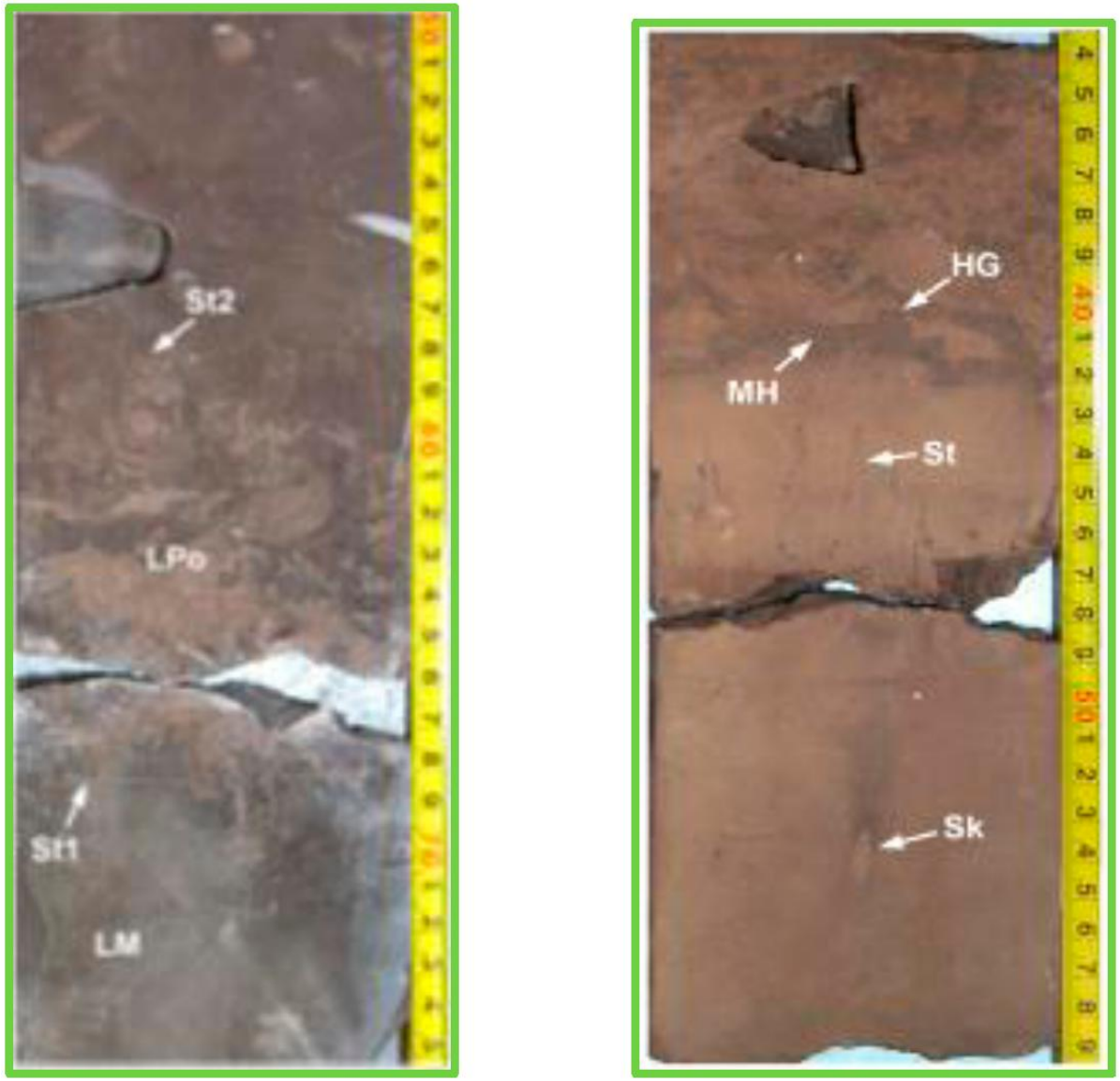

Figure 9. A) (left) Light-medium grey, peloidal lime mudstone (LM), transitional up to wackestone which is overlain by medium-coarse oolitic packstone (LPo) with calcite-cemented grainstone pockets. Two well-developed stylolites (St) are observed. B) (right) Very fine to fine, slightly dolomitic peloidal packstone with sub-vertical *Skolithos* burrows (Sk) overlain by micritic wackestone horizon (MH) capped by irregular hardground (HG) overlain by slightly dolomitic packstone. Note major stylolite (St).

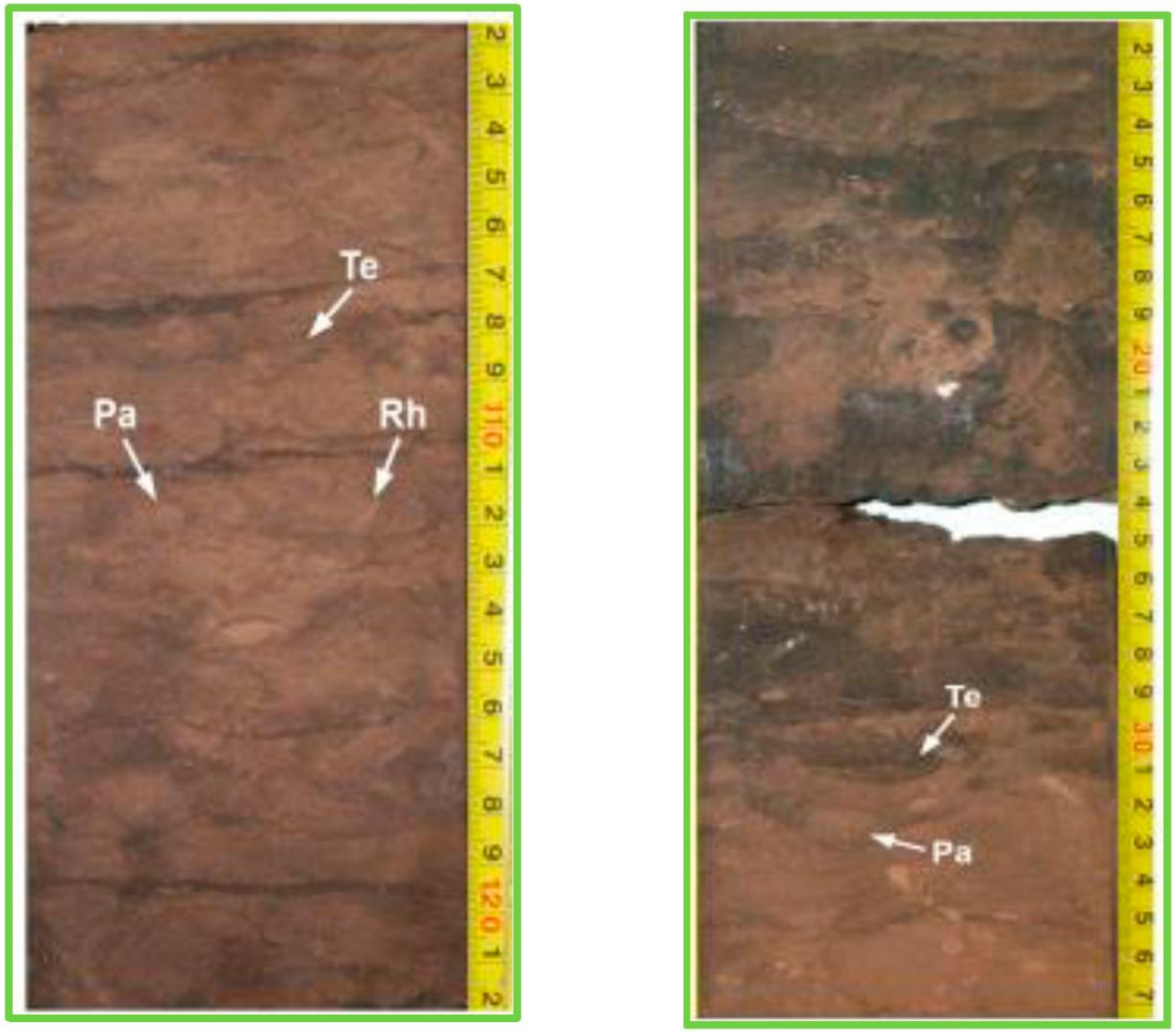

Figure 10. A) (left) Rarely porous, slightly argillaceous bioturbated dolowackestone becoming transitional to dolomitic oncoidal wackestone. Burrow structures include *Teichichnus* (Te), *Paleophycus* (Pa) and possibly *Rhizocorallian* (Rh). B) (right) Very finely crystalline, sucrosic, bioturbated, slightly argillaceous dolomitic wackestone with fair matrix intercrystalline porosity containing dark brown bitumen stain. Burrow structures are mainly *Teichichnus* (Te) and *Paleophycus* (Pa).

Figure 11. A) (left) This view shows well indurated, tight, faintly burrow mottled slightly argillaceous lime mudstone with few dark pyritized grains (DG). B) (right) Very fine to coarse, locally argillaceous, oncolitic dolomitic wackestone. Oncoids (On) are mostly non-dolomitic but contain dolomitic microporous layers within central cores. White area (An) is a small anhydrite nodule.

Figure 12. A) (left) This view shows greyish brown, slightly dolomitic lime mudstone with irregular fissure structures (FS) infilled with argillaceous grainy wackestone. B) (right) This view shows algal laminate with common reworking of laminae in a supratidal environment. Note mm-scale algal laminae (Al) and common very coarse to pebble-sized intraclasts (IC).

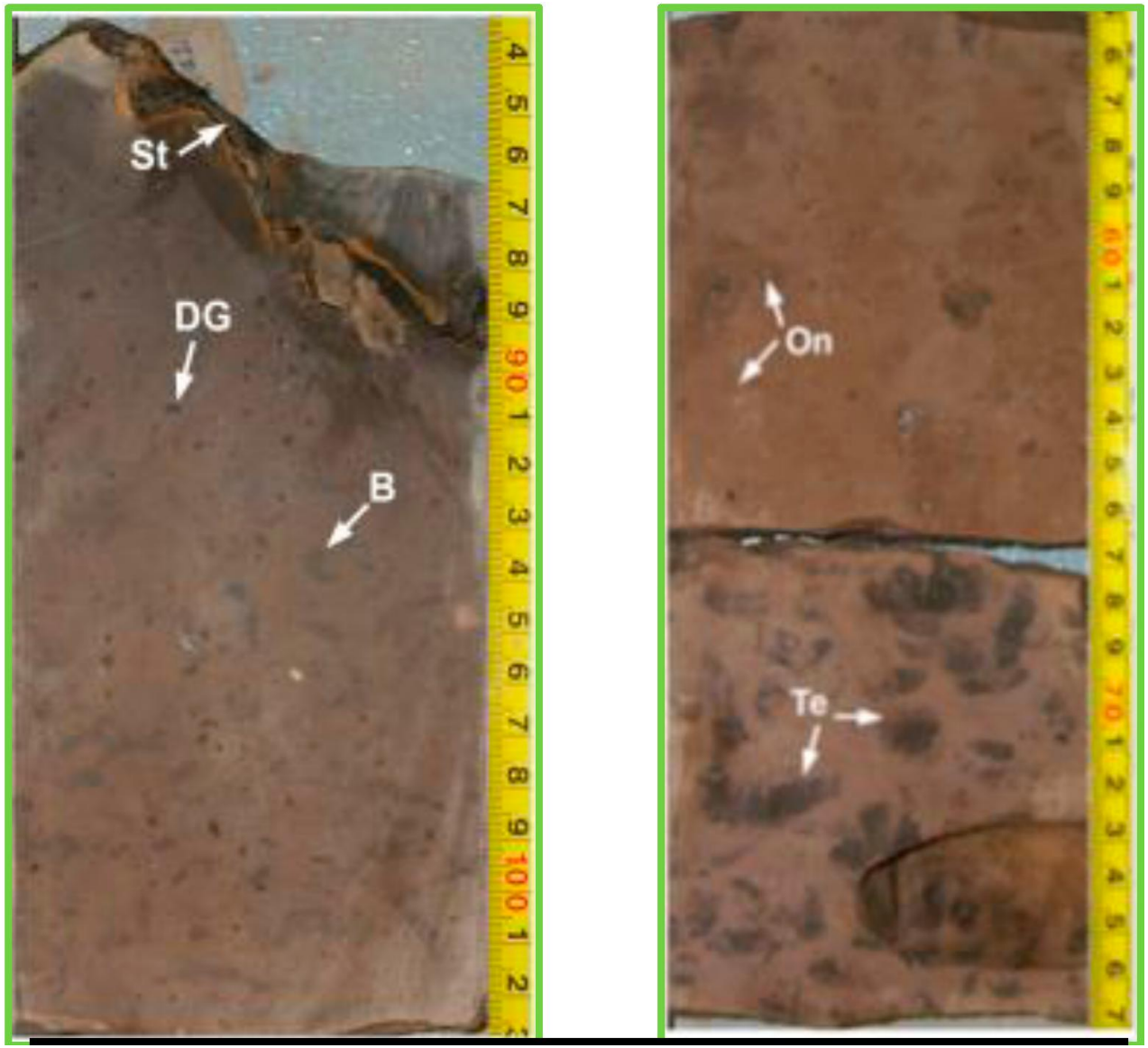

Figure 13. A) (left) Light greyish brown mottled, possibly slightly dolomitic bioturbated lime mudstone with dark pyritized burrow structures (B) and moderate dark pyritized oncoidal grains and peloids (DG). Note prominent stylolite (St). B) (right) Very fine dolomitic wackestone with common bitumen-stained *Teichichnus* burrows (Te). The overlying core piece contains upward increasing small oncoids/coated grains (On).

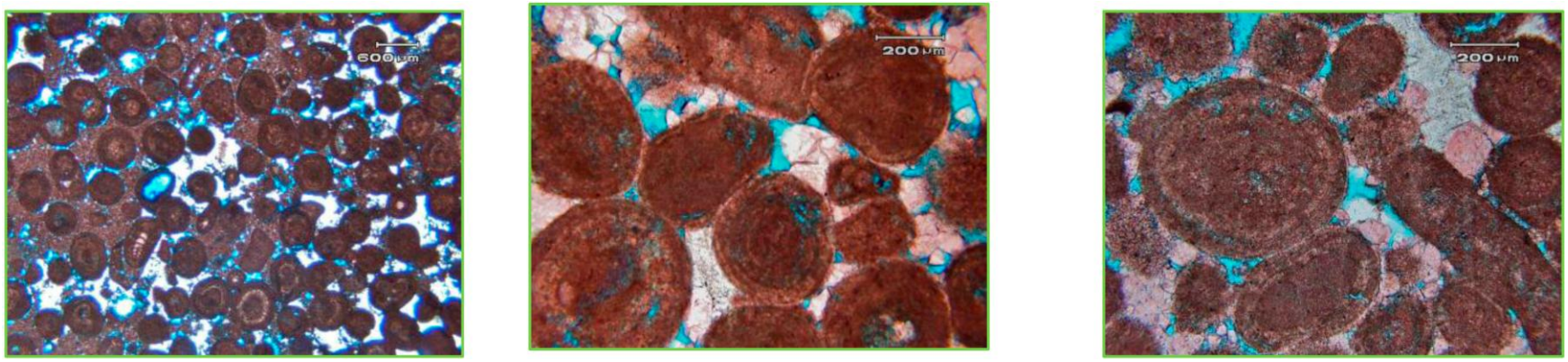

Figure 14. A) (left) Fine rim of bladed calcite coats ooids. Then sparse fine-medium equant calcite (pink) reduced interparticle pores in oolitic grainstone. B) (middle) This image emphasizes the partly-leached ooid cortices. Some of the leaching was obviously very fabric selective. These were finally filled by coarse baroque dolomite. C) (right) Thin isopachous calcite rims on the ooids and the medium crystalline calcite spar cement that reduces interparticle porosity within the grainstone.

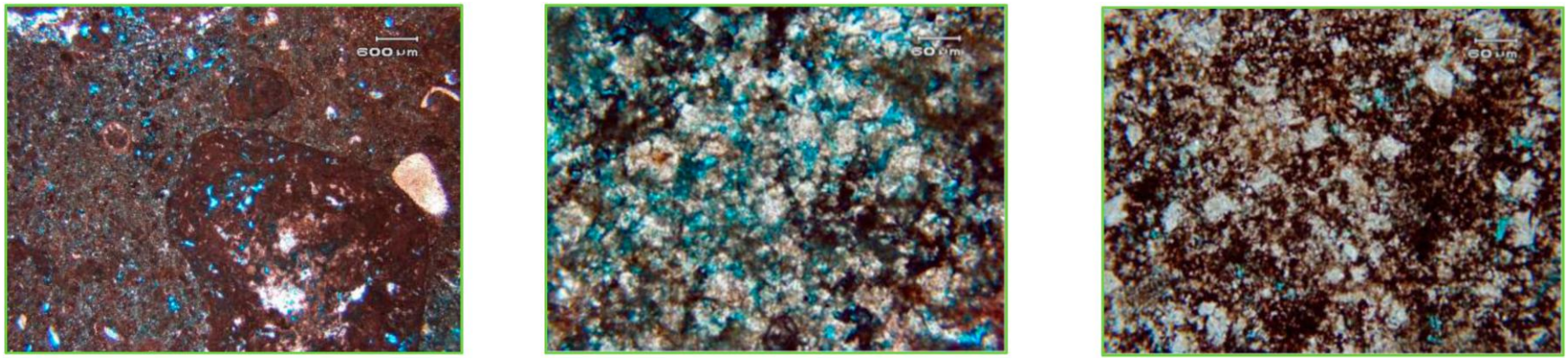

Figure 15. A) (left) Dolomitization has replaced much of the matrix with fine dolomite in oncolitic wackestone. Fine equant dolomite and calcite crystals partly cement the small moldic pores. B) (middle) Dolomitization has replaced much of the matrix with medium to fine dolomite. C) (right) Fine to medium crystalline dolomite has pervasively replaced the fabric of this sample. This resulted in a good intercrystalline matrix pore system prior to hydrocarbon migration and bitumen cements being formed.

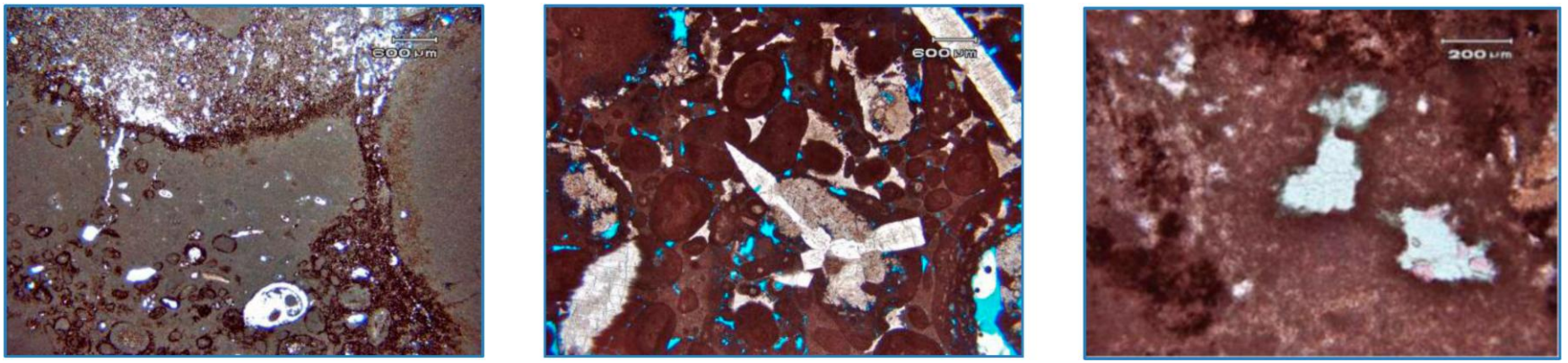

Figure 16. A) (left) Peloidal packstone. This is a calcrete/soil horizon where the basic microfacies has been altered by micritization, allochem leaching, infilling with argillaceous and some bituminous material. During exposure, corrosion of vugs occurred, subsequently vugs were filled by an argillaceous residual (soil). B) (middle) Oolitic packstone. Coarse dolomite is inclusion rich and primarily filled interparticle spaces. Late-stage euhedral anhydrite cement (white) in part replaced dolomite and clearly post-dates the dolomite. C) (right) Oncolitic wackestone. Sparry calcite cement and coarse quartz cement (white) fills moldic pores within the oncoid structure. There are some dolomite inclusions within the quartz indicating that they were largely replaced. The partial dolomitization of matrix and dolomitic sediment infill of moldic cavities within the oncoid indicates its paragenetically early origin.

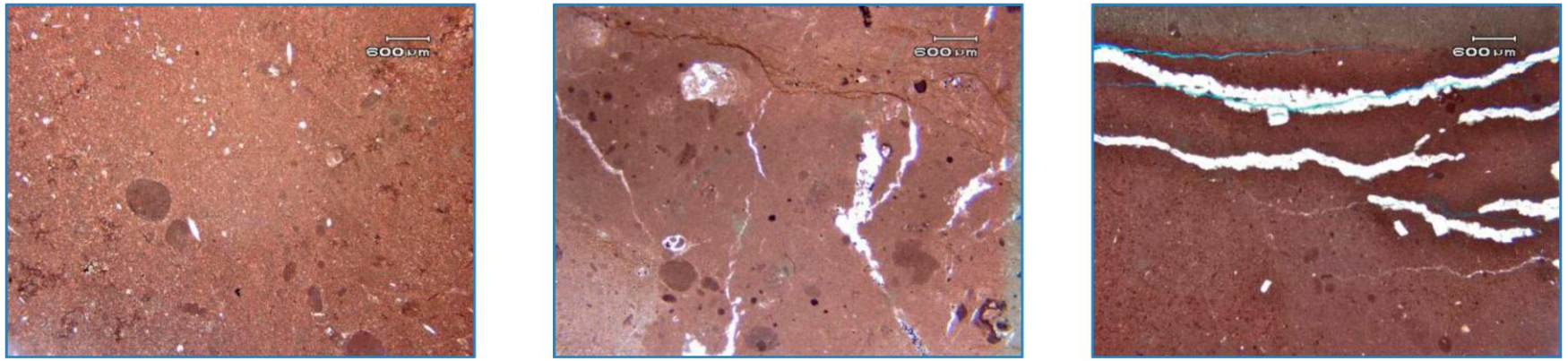

Figure 17. A) (left) Partial dolomitization of matrix and neomorphism of matrix to microspar is observed in lime mudstone. B) (middle) Discontinuous fractures (white) that occur in the matrix of lime mudstone and are oriented at a high angle to bedding are completely filled with medium- to coarse-crystalline calcite cement. C) (right) Two generations of fractures are seen within Lime Mudstone matrix. Anhydrite-cemented first generation fractures and matrix are cut by second generation hairline fractures.

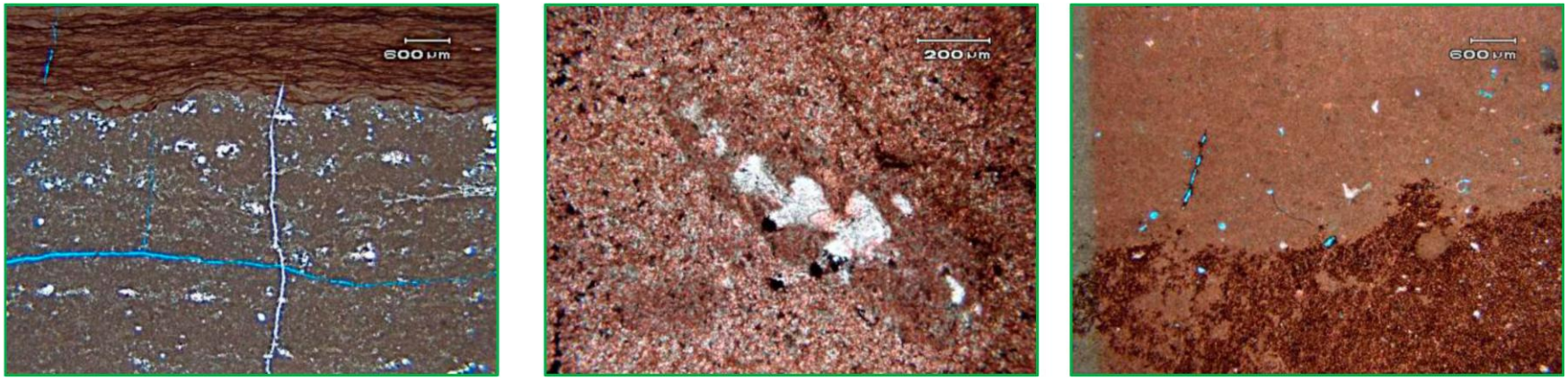

Figure 18. A) (left) Note two high angle fractures. Fracture on left is open; on right fracture is cemented by fine calcite. B) (middle) Tiny non-touching moldic pores in matrix. C) (right) Small non-touching moldic pores (Facies Association MMF5).

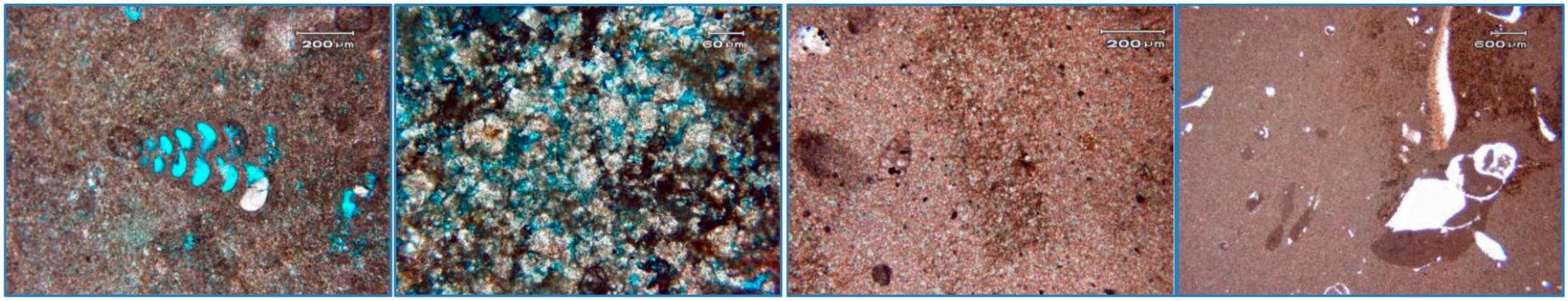

Figure 19. A) (left) Intraparticle porosity in the open chambers (in blue) of a foram in oncoidal packstone (MMF2). B) (middle) Intercrystalline porosity between fine to medium dolomite crystals in the matrix of oncolitic wackestone (MMF2). C) (3rd from left) Medium to coarse calcite cementation, partial pyrite replacement of matrix and compaction has completely destroyed porosity in wackestone (MMF3). D) (right) Laths of replacement anhydrite scattered through burrows and matrix of lime mudstone, no visual porosity (MMF4).

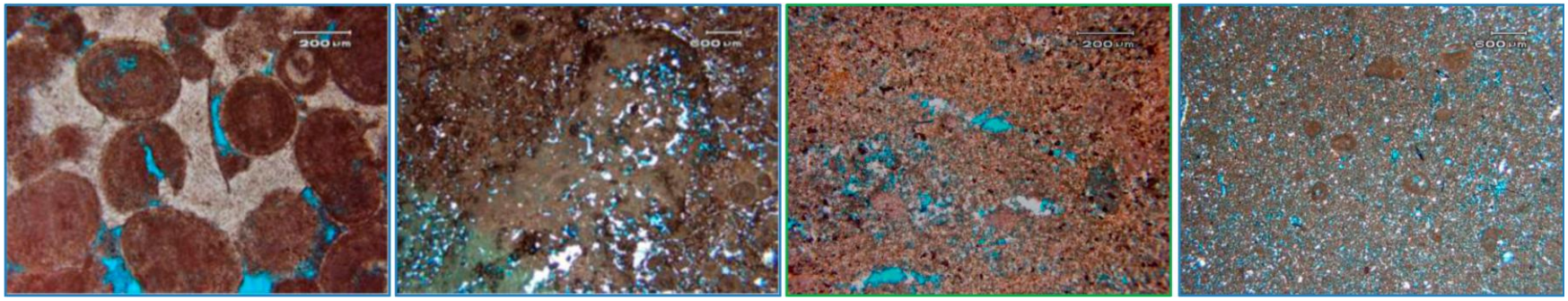

Figure 20. A) (left) Interparticle porosity (in blue) in oolitic grainstone (MMF1). B) (middle) Interparticle and moldic porosity in packstone (MMF1). C) (3rd from left) Wackestone with moldic and well-connected matrix intercrystalline porosity (MMF1). D) (right) Interparticle and moldic porosity in packstone (MMF2).